Full Paper

Essential Oil of *Aaronsohnia Pubescens* Subsp. *Pubescens* as Novel Eco-Friendly Inhibitor for Mild Steel in 1.0 M HCl

Mounir Manssouri,[1,*] Mohamed Znini,[1] Yassir El Ouadi,[2] Abdeslam Ansari,[1] Jean Costa[3] and Lhou Majidi[1]

[1]*Moulay Ismail University of Meknes, Laboratory of Natural Substances & Synthesis and Molecular Dynamics, Faculty of Sciences and Techniques, P.B 509, 52000, Errachidia, Morocco*
[2]*Laboratory of Analytical Chemistry, Materials, and Environment (LC2AME), Faculty of Sciences, University of Mohammed Premier, B.P. 717, 60000 Oujda, Morocco*
[3]*University of Corsica, CNRS-UMR 6134, Laboratory of Chemistry of Natural Products, BP 52, 20250 Corti, France*

*Corresponding Author, Tel.: + 212 (06)99400646
E-Mail: man.mounir@yahoo.fr

Abstract- The essential oil from the aerial parts of *Aaronsohnia pubescens* subsp. *pubescens* plant (*APS* oil) was extracted by hydrodistillation, and then its composition was analyzed by gas chromatography (GC) and GC-mass spectrometry (GC/MS). We identified thirty-four constituents presenting 87% of the total amount, Which, Carvacrol (13.9%), α-Pinene (10.3 %), E-Anethole (10.1%) and Ar-Turmerone (9.3%) were identified as major constituents of *APS* oil. The corrosion inhibition and adsorption (CIA) performance of the *APS* oil on the corrosion mild steel (MS) in 1M hydrochloric acid was evaluated by the weight loss (WL) analysis and electrochemical assays. The weight loss outcomes indicate that *APS* oil shows a worthy inhibitory efficiency of 89.88 % which reached at 3g.L^{-1} and 343 K. The charge transfer process mainly controls the results of EIS measurements, PDP measurements showed that the studied *APS* oil performs as a mixed-type inhibitor. Furthermore, the adsorption on the MS surface follows the Langmuir model.

1. INTRODUCTION

In recent years, the MS corrosion has turned the interest of the corrosion scientists for discovering the newly materials which have capability to protect it to the corrosion [1,2]. In this sense, to eliminate the undesirable scales and corrodes which ousted on the MS surface, the two acids hydrochloric and sulphuric are frequently used for this purpose [3]. Nevertheless, due to the thermodynamic instability of MS, especially which in contact with the aggressive solution medium, it becomes very disposed to the corrosion [4]. Hence, the reduced corrosion resistance of MS in acidic solutions needs to add corrosion inhibitors which act by chemical and/or physical adsorption to limit its attack [4]. Organic compounds act as the best way to prevent the corrosion of metal surfaces due to existence of unsaturated bonds and/or hetero atoms as well as the reactive functional groups in their structures [5,6].

Almost all inhibitors of corrosion are synthetic organic compounds [7,8], but these compounds are often considered as highly toxic species and not eco-friendly with environment. At this time, using non-hazardous and natural inhibitors become very important because of their environmentally eco-friendly nature [9,10]. Recently, a great deal of research has been carried out to study inhibitive effect several plant extract on the corrosion of steel in 1 M HCl [11–15]. In this work, our focus is chiefly put on the EO of *Aaronsohnia pubescens* subsp. *pubescens* (Fig. 1).

A.pubescens (Desf.) K. Bremer &Humphries is botanically a synonym of Matricaria pubescens (Desf.) Schultz. It is a pleasant-scented annual plant endemic to North Africa [16] and the CanaryIslands [17]. It is primarily found in non-saline wadis on preferably sandy-loamy soils. Parts of the plant are used in local folk medicine: In Morocco, this species, known locally as "*Taraght*", decoctions of the aerial flowering parts are used as mouthwash against toothache [18].

Fig. 1. *Aaronsohnia pubescens* subsp. *pubescens* in its native habitat in south-eastern of Morocco (Jorf-Errachidia)

The plant is also used as a food additive for flavoring and preservation purposes [16,18]. In both Algeria and Morocco, infusions of the aerial parts are used against gastric ulcers, flatulence, respiratory disorders, fever and rheumatic diseases [19]. To our knowledge, no study was published to study on inhibitive action of *APS* oil on corrosion of MS in 1M HCl solution. Therefore, this study is aimed; i) a determination of the chemical composition of studied *APS* oil using gas chromatography (GC) and GC-mass spectrometry (GC/MS), ii) an investigation the inhibitory action of *APS* oil using the monitory techniques such as low weight measurements and electrochemical methods.

2. EXPERIMENTAL

2.1. *APS* oil isolation

The aerial parts of Aaronsohnia pubescens *subsp*. pubescens were collected in May and June 2018 (full bloom) in Errachidia, Morocco. Coupon specimens were deposited in the herbarium of the Faculty of Sciences and Technology of the same city. After that, 100 g of fresh plant material (100g) was subject to hydrodistillation for three hours using a Clevenger-type apparatus according to the method recommended in the European Pharmacopoeia [20] and the EO yield was 0.7%.

2.2. *APS* oil characterization

The analysis of *APS* oil was carried out by GC and GC-MS according to the described methodologies in our previous work [21-23], using a Perkin-Elmer Autosystem XL GC apparatus. Fused-silica capillary columns (60 m×0.22 mm i.e., film thickness 0.25 µm), Rtx-1 (polydimethylsiloxane) and Rtx-wax (polyethyleneglycol). Temperature program: from 60 °C to 230 °C at 2 °C/min and then held isothermally at 230 °C for 35 min. Injector and detector temperatures were held at 280 °C. Samples were injected in the split mode (1/50), the carrier gas was H_2 (1 ml/min); the volume injected was 0.2 µl of pure oil. MS conditions: Turbo mass detector quadrupole, EI+=70 eV, acquisitions scan mass range of 35-350 Da, split: 1/80, injection volume: 0.2 µl of pure oil.

2.3. Preparation of MS segments, corrosive solutions and inhibitors

Corrosion tests were realized on the MS segments with dimension of 2 cm×2 cm×0.05 cm; the MS metal presents the subsequent composition with mass percentage (%): P 0.09, Si 0.38, Al 0.01, Mn 0.05, C 0.21, S 0.05 and Fe 99.21. The corrosive acid solution is a 1 M of HCl, was prepared from HCl (37%) by dilution with distilled water.

2.4. Corrosion monitoring techniques

2.4.1. Weight loss (WL) measurements

The prepared MS segments are weighed; then they are immersed in 1M HCl with and without different concentrations between 0.25 and 3 g.L^{-1} of *APS* oil under different temperatures of 308 to 343 K after an exposure time of six hours [24]. Inhibitory efficiency (*IE %*) is determined basing on the MS corrosion rates *W* (mg.cm^{-2}.h^{-1}) according to the subsequent relationship [25] (Eqs. 1,2):

$$W = \frac{m_f - m_i}{S.t} \tag{Eq. 1}$$

where m_i and m_f (mg) is the MS segment weight before and after immersion in the tested solution. *S* is the area of the MS segment (cm^2) and *t* is the exposure time (h).

$$IE\% = \frac{W - W'}{W} \times 100 \tag{Eq. 2}$$

With W and W' are the MS corrosion rates in both uninhibited and inhibited solution, respectively. The extent of the surface coverage (θ) is defined as follows [26] (Eq. 3):

$$\theta = \frac{IE\%}{100} \tag{Eq. 3}$$

2.4.2. Electrochemical (PDP and EIS) measurements

PDP and EIS measurements were performed used utilizing an assembly of electrochemical cell containing three electrodes: a disc cut form of MS as working electrode (1cm^2), a saturated calomel electrode as a reference electrode and a platinum electrode as against electrode. All electrochemical measurements were carried out using a potentiostat/galvanostat (Model 263A) and the electrochemical parameters values were determined using the Volta Master 4 software. We note that all potentials measurements in this study were obtained with respect to the potential value of reference electrode. The PDP tests are achieved in 1M HCl and in various concentrations of *APS* oil (0.25 to 3g.L^{-1}) at the temperatures range of 308 to 343 K, simultaneously. Furthermore, the cathodic and anodic curves are plotted by varying the electrode potential between -800 to +800 mV versus reference electrode at open circuit potential with a scan rate of 0.5 mV/sec. Inhibitory efficiency E$_{PDP}$ (%) is determined basing on the current corrosion I of MS at the above conditions according to the ensuing relationship (Eq. 4):

$$E_{PDP}(\%) = \left(\frac{I_{corr} - I_{corr,inh}}{I_{corr}} \right) \times 100 \tag{Eq. 4}$$

where I$_{corr}$ and I$_{corr,inh}$ are the corrosion current densities in the absence and the presence of inhibitor, respectively. Total charge transfer resistances R$_t$ (in the absence of inhibitor) and R$_t^{'}$

(in the presence of inhibitor) were calculated from Nyquist plots by measuring the impedance difference at low and high frequencies. The protective effectiveness E_{EIS} (%) using the following equation (Eq. 5):

$$E_{EIS}(\%) = \left(\frac{R'_t - R_t}{R'_t}\right) \times 100 \qquad \text{(Eq. 5)}$$

According to constant phase element (*CPE*) that accounts for the heterogeneities surface via the n coefficient [27], *ZCPE* impedance is determined as follows (Eqs. 6-8):

$$Z_{CPE} = Q^{-1}(i\omega)^{-n} \qquad \text{(Eq. 6)}$$

where Q is the constant of the CPE, ω is the angular frequency and n is the phase shift

$$C_{dl} = (Q \times R_{ct}^{1-n})^{\frac{1}{n}} \qquad \text{(Eq. 7)}$$

$$\omega = 2\pi\, f_{max} \qquad \text{(Eq. 8)}$$

f_{max} is the frequency for which the imaginary part of the impedance is maximum.

The C_{dl} (capacity of the double layer) is determined from the CPE as following equation:

$$C_{dl} = \frac{1}{2.\pi.f_{max}.R_t} \qquad \text{(Eq.9)}$$

3. RESULTS AND DISCUSSION

3.1. Chemical composition of *APS* oil

The chemical composition of *APS* oil was obtained from GC and GC-MS techniques. thirty-four components were characterized, which accounted to 87% of the total oil (Table 1). Hence, the dominant components of APS oil were established with mass percentage as follows: six hydrocarbon monoterpenes (17.3%), thirteen oxygenated monoterpenes (31%), one hydrocarbon sesquiterpene (0.6%), one oxygenated sesquiterpene (9.3%), seven nonterpenic oxygenated compounds (12.9%) and six other compounds (15.9%). Among them, Carvacrol (13.9%), α-Pinene (10.3%), E-Anethole (10.1%) and Ar-Turmerone (9.3%) were identified as major constituents of APS oil (Table 1).

3.2. Corrosion and adsorption behavior of *APS* oil on MS surface in 1 M HCl

3.2.1 Weight loss analysis, kinetic and thermodynamic parameters

3.2.1.1 Effect of *APS* oil concentration and temperature media

This paragraph aimed to study the influence of *APS* oil concentration and temperature media on the progress of corrosion rate of MS and the inhibitory efficiency related to the *APS* oil in corrosive media (1M HCl) at range temperature of 308 to 343K in the absence and presence of different concentrations of *APS* oil.

Table 1. Chemical composition of the *APS* oil from south-eastern of Morocco

N [a]	Components[b]	RI a [c]	RI p [d]	% HD [e]
1	α-Pinene	931	1018	**10.3**
2	β -Pinene	971	1107	2.8
3	α-Phellandrene	998	1159	0.5
4	P-Cymene	1013	1262	2.3
5	Limonene	1021	1195	1.1
6	Cineole 1.8	1021	1205	3.9
7	Z-β-Ocimene	1026	1227	0.3
8	Fenchone	1069	1426	0.2
9	Ethyl heptanoate	1080	1325	0.4
10	Linalool	1085	1535	0.7
11	Camphre	1122	1502	1.3
12	Terpinen-4-ol	1163	1588	1.1
13	α -Terpineol	1174	1687	2.3
14	Estragole	1176	1653	1.3
15	Ethyl octanoate	1180	1426	0.3
16	Cuminaldehyde	1227	1762	2.0
17	p-Anisaldehyde	1220	2054	2.0
18	Perillaldehyde	1257	1760	1.5
19	**E-Anethole**	**1277**	**1807**	**10.1**
20	Thymol	1269	2158	1.8
21	2-Undecanone	1274	1590	1.2
22	**Carvacrol**	**1277**	**2193**	**13.9**
23	α-Terpinyl acetate	1331	1656	0.8
24	p-Acetonylanisole	1343	2100	1.3
25	Acid Decanoic	1353	1474	1.0
26	Methyl Eugenol	1366	1994	0.6
27	Ethyl decanoate	1382	1629	2.5
28	E-Caryophyllene	1416	1588	0.6
29	Dill apiol	1591	2350	0.6
30	t-Cadinol	1623	2149	0.8
31	β-Eudesmol	1634	2243	0.7
32	**Ar-Turmerone**	**1634**	**2229**	**9.3**
33	(E)-heptadeca-10. 16-dien-7-one	1825	2213	6.4
34	Ethyl hexadecanoate	1977	2230	1.1
	Total			**87.0**
	Monoterpene Hydrocarbons			**17.3**
	Oxygenated monoterpenes			**31.0**
	Sesquiterpene Hydrocarbons			**0.6**
	Oxygenated sesquiterpenes			**9.3**
	Phenylpropanoids			**15.9**
	Oxygenated non-terpenic compounds			**12.9**

[a] Order of elution is given on apolar coloumn (Rtx-1)
[b] Normalized % abundances of oil are given on the apolar column
[c] Retentionindices on the Rtx-1 apolarcolumn
[d] Retentionindices on the Rtx-wax polarcolumn
[e] Percentage composition is given on the apolar column

Then, the results (Table 2) show that the protective effectiveness IE% goes up considerably with the increase in concentration of *APS* oil, indicating that the extent of inhibition depends on the concentration of this inhibitor. Besides, we notice that these findings demonstrate that the effectiveness IE% depends on the temperature and increases slightly when it rises from 308 to 343 K. More than that, when the concentration reached to 3 g/L, the effectiveness IE% reached a high value of 89.88 % in 1 M HCl solution at 343 K. Such behavior can be explained by adsorption coverage of *APS* oil on the metal surface that increases with concentration of inhibitor.

Table 2. Weight loss results of diverse concentrations of *APS* oil in 1 M HCl at various temperatures

	C(g.L^{-1})	*W*(mg.cm^{-2}.h^{-1})	*IE %*	*θ*
T = 308 K	0.00	0.942	-	-
	0.25	0.346	80.01	0.8001
	0.50	0.297	84.33	0.8433
	1.00	0.282	85.43	0.8543
	2.00	0.177	86.01	0.8601
	3.00	0.160	87.07	0.8707
T = 313 K	0.00	0.641	-	-
	0.25	0.641	80.06	0.8006
	0.50	0.548	84.79	0.8479
	1.00	0.512	85.61	0.8561
	2.00	0.322	86.07	0.8607
	3.00	0.290	88.17	88.17
T = 323 K	0.00	2.836	-	-
	0.25	1.031	81.18	0.8118
	0.50	0.886	84.89	0.8489
	1.00	0.825	85.77	0.8577
	2.00	0.514	86.12	0.8612
	3.00	0.465	88.67	0.8867
T = 333 K	0.00	3.641	-	-
	0.25	1.320	81.22	0.81.22
	0.50	1.134	84.93	0.84.93
	1.00	0.984	86.01	0.8601
	2.00	0.655	86.25	0.8625
	3.00	0.591	88.78	0.8878
T = 343 K	0.00	6.301	-	-
	0.25	2.271	81.55	0.8155
	0.50	1.893	84.96	0.8496
	1.00	1.670	86.32	0.8632
	2.00	1.085	86.97	0.8697
	3.00	1.010	**89.88**	**0.8988**

3.2.1.2 Kinetic and thermodynamic parameters

Basing on the famous rule of Arrhenius, we calculated standard activation energy E_a under temperature range of 308 to 343 K, with and without inhibitor concentration of 3 g.L^{-1}

of *APS* oil using relationship (Eq. 10) [28]. Then, we calculated the standard activation energies of enthalpy ΔH_a and ΔS_a using the relationship (Eq. 11) and (Eq. 12), respectively [29].

$$\ln W = \ln A' + \left[-\frac{E_a}{R\,T} \right] \tag{Eq. 10}$$

$$W = \frac{R.T}{N_a h} \exp\left[\frac{\Delta S_a^\circ}{R}\right] . \exp\left[-\frac{\Delta H_a^\circ}{R\,T}\right] \tag{Eq. 11}$$

$$\ln\left[\frac{W}{T}\right] = \ln\left[\left(\frac{R}{N_a h}\right) + \frac{\Delta S_a^\circ}{R}\right] + \left[-\frac{\Delta H_a^\circ}{R\,T}\right] \tag{Eq. 12}$$

where W, R, T, h, N_a and A' signify the corrosion rate, the universal constant of the ideal gas, the absolute temperature, the Plank constant, universal Avogadro number and the Arrhenius pre-exponential factor, respectively.
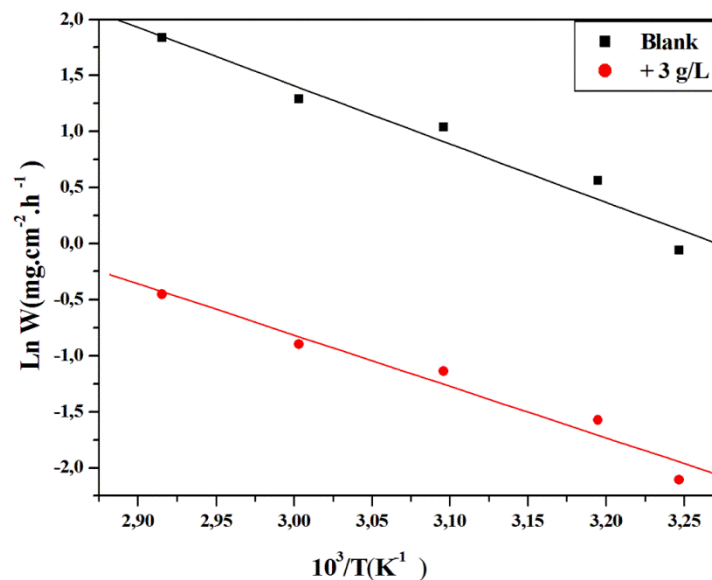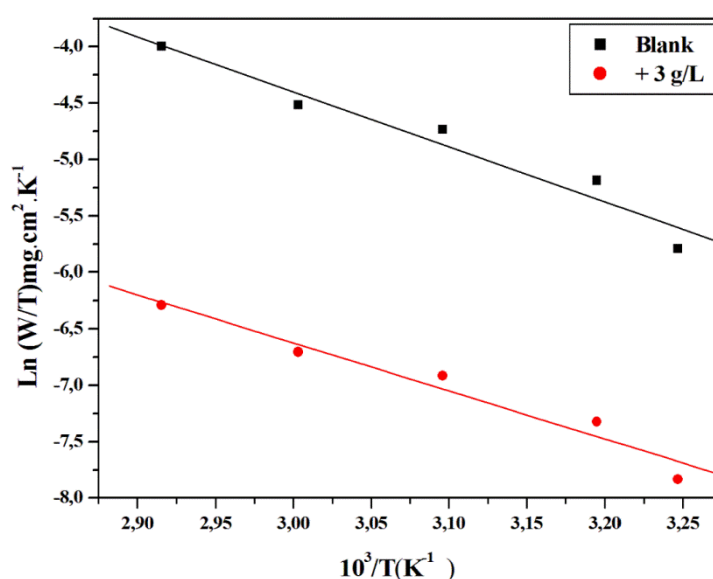

Fig. 2. Arrhenius plots in 1M HCl without and with APS oil (3 g.L^{-1}) under various temperatures

The plot corresponds to the variation of ln(W) versus (1000/T) for MS corrosion in 1M HCl with and without various concentrations of APS oil is displayed in Fig. 2. Moreover, the variation of ln(W/T) as function 1000/T for MS corrosion in 1M HCl with and without various inhibitor concentrations is shown in Fig. 3. Basing on the Fig.2 we have calculated the standard activation energy E_a, and then according to the Fig. 3 we have calculated standard activation enthalpy ΔH_a°, entropy ΔS_a° energies and the difference $E_a - \Delta H_a^\circ$ (Table 3). Accordingly, we observed that the activation energy attained in HCl (corrosive media) with of APS oil is less than that when the HCl is added alone; indicating clearly the chemisorption behavior of adsorption between MS surface and inhibitors species of APS oil [30]. In the other words, we found that the average difference Ea– ΔH_a° (2.7 kJ.mol^{-1}) is

almost equal to the average value of RT at the average temperature of 324 °K calculated in the studied domain which sustains that the corrosion process is uni-molecular reaction by the known of a perfect gas [31].

Additionally, the positive value of standard activation enthalpy indicate the endothermic dissolution phenomenon of MS [32]. Then, the negative value of the standard activation entropy exhibited a low disorder of the species well-thought-out in the studied adsorption [33]. We advance highlighted the low value of the standard activation entropy in the presence of inhibitory *APS* oil with respect to that when the solution contents only the HCl; revealing clearly the important role of *APS* oil inhibitor to reduce the disorder property related to the species which enter in adsorption system.

Fig. 3. Transition-state plots in 1M HCl without and with *APS* oil (3 g.L^{-1}) under various temperatures

Table 3. Kinetics thermodynamic for MS in 1 M HCl with and without APS oil (3 g.L^{-1})

C (g/L)	E_a (kJ. mol^{-1})	$\Delta H_a°$ (kJ. mol^{-1})	$\Delta S_a°$ (J. mol^{-1}.K^{-1})	E_a- ΔH_a (kJ. mol^{-1})
Blank (1M HCl)	43.35	40.65	-112.29	2.70
3.00	38.19	35.49	-146.31	2.70

3.2.1.3 Adsorption isotherm

To get information about the adsorption mechanism of the APS oil on the MS surface, adsorption isotherm models were used as Langmuir, Temkin, Frumkin and Freundlich (Eqs. 13, 14 and 15). Accordingly, we observed that the adsorption of APS oil on the MS surface obeys a Langmuir adsorption isotherm (Fig. 4).

Langmuir : $\frac{C}{\theta} = \frac{1}{K_{ads}} + C$ (Eq. 13)

Temkin : $\ln\left[\frac{C}{\theta}\right] = \ln K_{ads} - g.\theta$ (Eq. 14)

Frumkin : $\ln\left[C.\left(\frac{\theta}{1-\theta}\right)\right] = \ln K_{ads} + g.\theta$ (Eq. 15)

where K_{ads} and g are the adsorption/desorption equilibrium constant and the adsorbate parameter, respectively.

Fig.4 shows the straight lines of C/θ with respect to *APS* oil concentration at different temperatures (308 to 348 K). The linear regression factor R^2 values are showed in Fig. 4. As observed in Fig. 4 the values of R^2 is almost equal to 1, indicating that the adsorption on the MS surface follows the Langmuir adsorption isotherm [34]. This findings suggests that the adsorbed molecules of *APS* oil occupy only one protective layer and that there are no interactions between the adsorbed species [28].
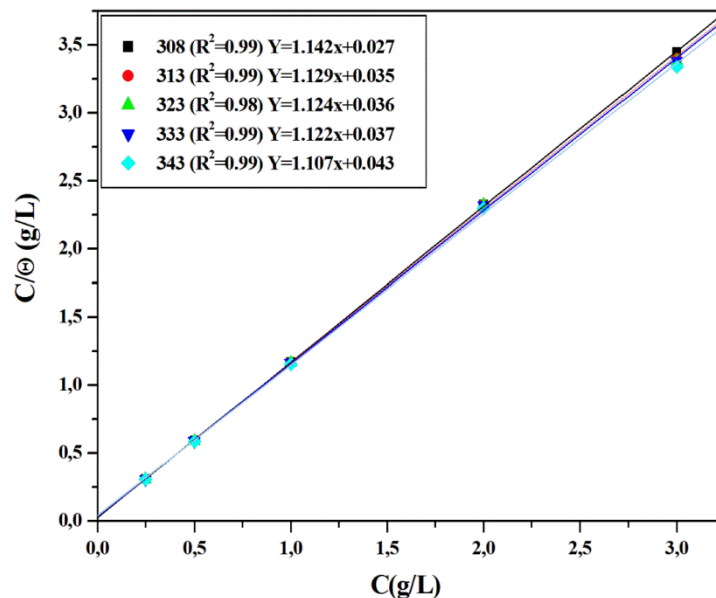

Fig. 4. Langmuir isotherm for *APS* oil adsorption on MS surface at 308 K

3.2.2 Electrochemical measurements (EIS and PDP)

3.2.2.1 EIS study

The evaluation of inhibition of APS oil to protect against corrosion of MS surface was carried by using EIS analysis. Fig.5 displays the Nyquist plots of MS after 30 min of immersion in 1M HCl in both with and without of various doses of *APS* oil at 308 K. As exposed in Fig.5, we perceived that the addition of the *APS* oil (0.25-3g.L^{-1}) to the corrosion medium clues to the rises of the size of the semi-circle diameters; highlighting the good inhibitory action of *APS* oil to prevents MS surface from corrosion.
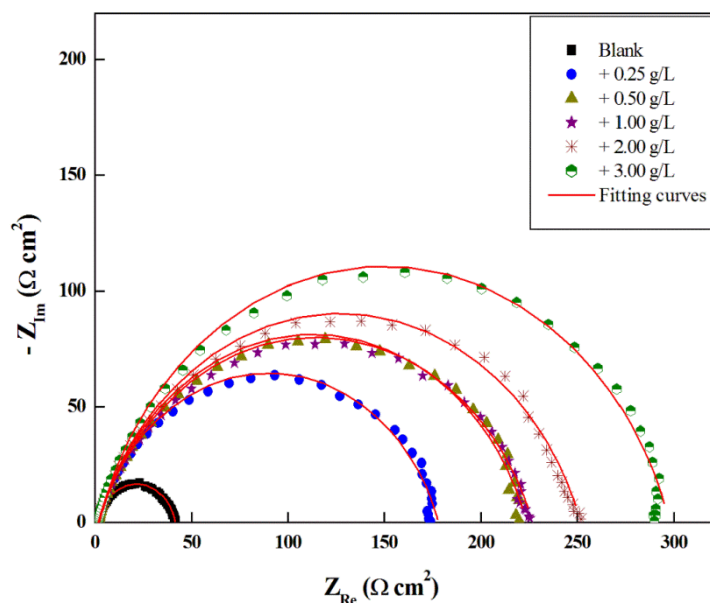
Fig. 5. Nyquist plots of MS in 1 M HCl in the absence and presence of various concentrations of *APS* oil at 308 K

Table 4. Parameters of EIS of MS in 1M HCl in the absence and presence of various concentrations of *APS* oil at 308 K

	C (g/L)	R_s (Ω cm²)	R_{ct} (Ω cm²)	C_{dl} (μFcm⁻²)	n_{dl}	Q (Ω^{-1} S^n cm⁻²)	Θ	EI$_{EIS}$ (%)
Blank (1M HCl)		1.80	40	65.60	0.888	127.9	-	-
	0.25	1.70	176	47.90	0.842	102.0	0.773	77.27
	0.50	2.20	222	45.60	0.826	93.3	0.819	81.98
APS oil	1.00	1.90	225	45.10	0.819	92.4	0.822	82.22
	2.00	1.80	250	38.50	0.834	91.1	0.840	84.00
	3.00	2.10	295	33.20	0.848	83.9	0.865	86.45

This inhibitory action of *APS* oil increases with the rises of its concentration, the same trends as those obtained from the low weight measurements. Moreover, the presence of a unique capacitive loop indicated that the studied adsorption is governed through a charge transfer process [35].

What is more is that, we noticed that the outputted impedance loops are not ideal semicircles, which mainly result to the surface irregularity, presence of crusts, and formation of spongy lattices.

An analysis of EIS leads us to calculate several parameters as solution resistance (*Rs*), charge transfer resistance (*Rct*), double layer capacitance (*Cdl*), and inhibitory efficiency (EI$_{EIS}$ %); these parameters are listed in Table 4.

Examination of the data in Table 4 show the R_t goes up and the C_{dl} goes down because of a decrease in local dielectric constant and/or an increase in the thickness of the electrical double layer. This can be attributed that there is an adsorption of the inhibitor molecules of APS oil on the MS surface forming a layer between the metal and the corrosives solution [36]. This finding suggests that the increase in the *APS* oil concentration increases the number of molecules adsorbed onto MS surface and to reduce the reactive sites which could be created during corrosion phenomenon.
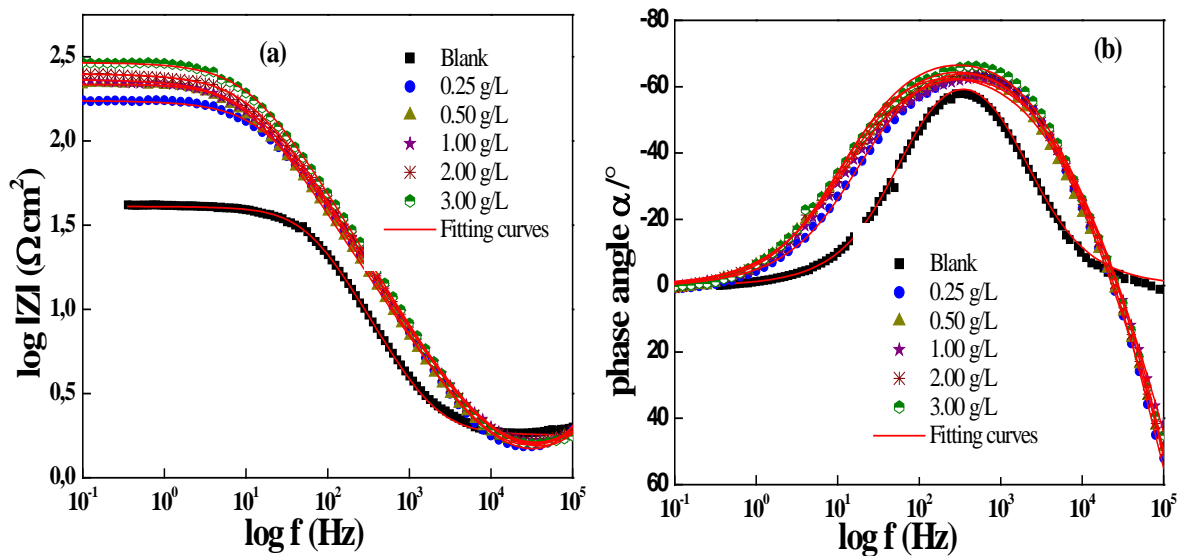
Fig. 6. Bode diagrams of MS in 1 M HCl before and after addition of TRC-H and TRC-Cl at 303 K

The highest inhibition efficiency 86.45 % was attained at 3 g. L^{-1} of *APS* oil. Fig. 6 shows the Bode plots of MS in 1M HCl in both uninhibited and inhibited solutions. To Fig. 6a, either at low, intermediate or high frequencies, we observed that the impedance plot rises with the increasing of concentration of *APS* oil and thus the above trends of inhibitory efficiency of *APS* oil is again confirmed. In the other words, Fig. 6b confirms evidently the existence of a single time constant and thus reconfirms the appearance of a single capacitive loop which explored by the Nyquist diagram [37].

Fig. 7, reveal an equivalent electrical circuit (EEC) of the MS/HCl/*APS* oil interface in wholly frequencies studied using the Ec-Lab software. EEC covering a constant phase element (CPE), the solution resistance (R_S), and the charge transfer resistor (R_{ct}).
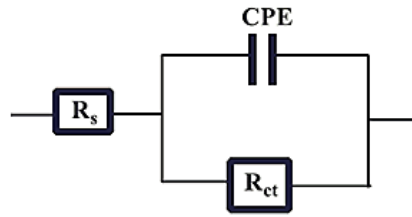
Fig. 7. EEC building of the interface: MS/HCl/*APS* oil

3.2.2.2 PDP study

PDP (anodic and cathodic) curves of MS in 1 M HCl out carried in the absence and presence of various concentrations of APS oil are exposed in Fig. 8.
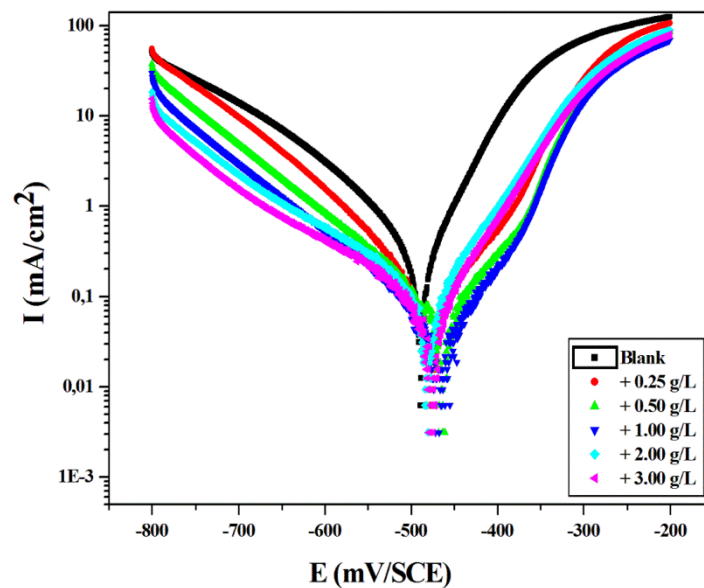
Fig. 8. Polarization curves of MS in 1 M HCl with and without *APS* oil at various concentrations at 308 K

From Fig. 8, we noticed that both cathodic and anodic curves were translated to lower current densities with an increase of *APS* oil concentration. This result can be attributed that there is an inhibition power of *APS* oil to stop oxidative and reductive reactions which could be caused the corrosion phenomenon on the MS surface. The calculated parameters of PDP analysis are summed up in Table 5.

It is crystal clear from the data in Table 5 attested that the corrosion current density I_{corr} decreases with increasing of APS oil concentration. Similarly, the EI_{PDP} (%) increases with increasing of APS oil concentration to reach its maximum value of 92.21 % at 3 g/L. These results suggested that APS oil is toughly adhered to the MS surface forming a protective layer, which stays electrochemical reactions to occur onto metal surface. Therefore, the maximum displacement for potential corrosion is 40 mV which indicates that the APS oil acts

as mixed-type inhibitor [38]. In this end, we have noticed that the applied techniques for corrosion tests of MS in 1M HCl as corrosive medium with *APS* oil concentration of 3 g.L^{-1} and temperature media of 308 K were significantly conducted to the high inhibitory efficiencies of *APS* oil, which approximately equals one to others.

Table 5. PDP parameters of MS in 1M HCl without and with different concentrations of *APS* oil at 308K

	C (g/L)	- E_{corr} (mV/SCE)	I_{corr} ($\mu A\ cm^{-2}$)	-βc (mV dec^{-1})	EI_{PDP} (%)
Blank (1M HCl)		490	578	148	-
APS oil	0.25	490	70	138	87.88
	0.50	460	68	140	88.23
	1.00	470	60	157	89.61
	2.00	470	55	156	90.48
	3.00	450	45	132	92.21

4. CONCLUSION

All in all, the *APS* oil has proved to be able to efficiently inhibit MS corrosion in 1M HCl solution; this EO attained its average high inhibitory efficiency of 87.07% at essential dose of 3 g.L^{-1} and temperature medium of 308 K. The adsorption of the RP oil not only was found to obey Langmuir isotherm but also showed a chemical interaction, which shows that the inhibition of corrosion can be attributed to the adsorption of EO main compounds such as, Carvacrol (13.9%), α-Pinene (10.3%), E-Anethole (10.1%) and Ar-Turmerone (9.3%). The Nyquist and Bode diagrams showed that adsorption mechanism of *APS* oil is governed by a charge transfer process. Furthermore, the natural oil acts as mixed type inhibitor.

REFERENCES

[1] A. Sedik, D. Lerari, A. Salci, S. Athmani, K. Bachari, İ.H. Gecibesler, and R. Solmaz, J Taiwan Inst. Chem. Eng. 107 (2020) 189.

[2] C.A. Loto, and R.T. Loto, J. Fail. Anal. Prev. 19 (2019) 1853.

[3] S. Lahrour, A. Benmoussat, B. Bouras, A. Mansri, L. Tannouga, and S. Marzorati, Appl. Sci. 9 (2019) 4684.

[4] D.K. Lavanya, F. V Priya, and D.P. Vijaya, J. Fail. Anal. Prev. 20 (2020) 494.

[5] M.Y. El Sayed, A.M. Abdel-Gaber, and H.T. Rahal, J. Fail. Anal. Prev. 19 (2019) 1174.

[6] G.A. Swetha, H.P. Sachin, A.M. Guruprasad, and B.M. Prasanna, J. Fail. Anal. Prev. 19 (2019) 1113.

[7] I. Merimi, Y. Ouadi, R. Benkaddour, H. Lgaz, M. Messali, F. Jeffali, and B. Hammouti, Mater Today Proc. 13(2019) 920.

[8] Y.E. Louadi, F. Abrigach, A. Bouyanzer, R. Touzani, and A. El Assyry, Port. Electrochim. Acta. 35 (2017) 159.

[9] Y. El Ouadi; A. Beladjila, A. Bouyanzer, Z. Kabouche, H. Bendaif, F. Youssfi, M. Berrabah, R. Touzani, A. Chetouani, and B. Hammouti, Mor. J. Chem. 5 (2017) 139.

[10] A. Chraka, I. Raissouni, N.B Seddik, S. Khayar, A.I. Mansour, S. Tazi, F. Chaouket, and D. Bouchta, J. Bio. Tribo. Corros, 6 (2020) 80.

[11] M. Manssouri, Y. El Ouadi, M. Znini, J. Costa, A. Bouyanzer, J.M. Desjobert, and L. Majidi, J. Mater. Environ. Sci. 6 (2015) 631.

[12] M. Manssouri, M. Znini, A. Ansari, A. Bouyenzer, Z. Faska, and L. Majidi, Der Pharma Chem. 6 (2014) 331.

[13] M. Znini, J. App. Chem. Env. Prot. 3 (2018) 1.

[14] M. Manssouri, A. Laghchimi, A. Ansari, M. Znini, Z. Lakbaibi, Y. El Ouadi, and L. Majidi, Mediterr. J. Chem. 10 (2020) 253.

[15] M. Manssouri, M. Znini, Z. Lakbaibi, Y. El Ouadi, and L. Majidi, Anal Bioanal Electrochem. 12(2020) 607.

[16] S. Benhouhou, Aaronsohnia pubescens (Dasf.) K. Bremer & Humphries. A Guide to Medicinal Plants in North Africa, Malaga (Spain), IUCN Centre for Mediterranean Cooperation (2005).

[17] J.A. Reyes-Betancort, S. Scholz, M.C.L. Arencibia, About the presence of the Moroccan endemic Aaronsohnia pubescens subsp. maroccana in the Canary Islands (Anthemidae, Asteraceae). Vieraea (2003).

[18] M. Abouri, A. El Mousadik, F. Msanda, H. Boubaker, B. Saadi, and K. Cherifi, Int J Med. Plants Res. 1 (2012) 99.

[19] M. Djellouli, A. Moussaoui, H. Benmehdi, L. Ziane, A. Belabbes, M. Badraoui, N. Slimani, N. Hamidi, Asian J. Nat. Appl. Sci. 2 (2013) 59.

[20] Council of Europe, European Pharmacopoeia, (3rd ed.) Strasbourg (1997).

[21] M. Manssouri, A. Ansari, M. Znini, L. Majidi, and J. Costa, Am. J. Innov. Res. Appl. Sci. 9 (2019) 57.

[22] M. Manssouri, M. Znini, and L. Majidi, J. Taibah Uni. Sci. 14 (2020) 124.

[23] M. Manssouri, A. Ansari, M. Znini, L. Majidi, and J. Costa, Egypt. J. Chem.63 (2020)51.

[24] Standard, A.S.T.M. G1-03. Standard practice for preparing, cleaning, and evaluating corrosion test specimens. Annual Book of ASTM Standards (2003).

[25] R. Nabah, F. Benhiba, Y. Ramli, M. Ouakki, M. Cherkaoui, H. Oudda, I. Warad, and A. Zarrouk, Anal. Bioanal. Electrochem. 10 (2018) 1375.

[26] A. Boumezzourh, M. Ouknin, E. Chibane, J. Costa, A. Bouyanzer, B. Hammouti, and L. Majidi, Int. J. Corros. Scale Inhib. 9 (2020) 152.

[27] A. Zarrouk, H. Zarrok, Y. Ramli, M. Bouachrine, B. Hammouti, A. Sahibed-Dine, and F. Bentiss, J. Mol. Liq. 222 (2016) 239.

[28] L. Messaadia, O. I. D. El Mouden, A. Anejjar, M. Messali, R. Salghi, O. Benali, O. Cherkaoui, and A. Lallam, J. Mater. Environ. Sci. 6 (2015) 598.

[29] S. Martinez, and I. Stern, Appl. Surf. Sci. 199 (2002) 83.

[30] A.M. Badiea, and K.N. Mohana, Corros. Sci. 51 (2009) 2231.

[31] S. Kharchouf, L. Majidi, M. Znini, J. Costa, B. Hammouti, and J. Paolini, Int. J. Electrochem. Sci. 7 (2012) 10325.

[32] I. El Ouali, B. Hammouti, A. Aouniti, Y. Ramli, M. Azougagh, E.M. Essassi, and M. Bouachrine, J. Mater. Environ. Sci. 1 (2010) 1.

[33] Y. El Ouadi, A. Bouyanzer, L. Majidi, J. Paolini, J.M. Desjobert, J. Costa, A. Chetouani, B. Hammouti, S. Jodeh, and I. Warad, Res. Chem. Intermed. 41 (2015) 7125.

[34] Y. Kharbach, F. Z. Qachchachi, A. Haoudi, M. Tourabi, A. Zarrouk, C. Jama, L.O. Olasunkanmi, E. E. Ebenso, and F. Bentiss, J. Mol. Liq. 246 (2017) 302.

[35] A.R. Sathiya Priya, V.S. Muralidharan, and A. Subramania, Corrosion. 64 (2008) 541.

[36] K. Juttner, Electrochim. Acta 35 (1990) 1501.

[37] D.K. Yadav, M.A. Quraishi, and B. Maiti, Corros. Sci. 55 (2012) 254.

[38] A. K. Satapathy, G. Gunasekaran, S. C. Sahoo, K. Amit, and P. V. Rodrigues, Corros. Sci. 51 (2009) 2848.